ISSN: 2181-3337 | SCIENTISTS.UZ VOLUME 5 ISSUE 8 AUGUST 2026

REVERSE OSMOSIS MEMBRANES UNDER DUTY-CYCLED OPERATION: COMPACTION, SCALING, BIOFILM REGROWTH AND PERMEATE TRANSIENTS IN PHOTOVOLTAIC-DRIVEN BRACKISH DESALINATION

Kuralov Murodbek[1], **Akhatov Jasurjon**[2]
PhD student, Corresponding author. makuralov@gmail.com[1]
Doctor of Technical Sciences, Professor[2]
S. A. Azimov Physical-Technical Institute, Academy of Sciences of the Republic of Uzbekistan, Tashkent, Uzbekistan

DOI: 10.67620/sai.58a0005

ABSTRACT

Photovoltaic-driven reverse osmosis is the dominant architecture for decentralised brackish-water supply in arid regions, yet it violates the condition under which almost all membrane performance data are obtained: steady pressure, steady flux and continuous operation. This review assembles the evidence on how the polyamide membrane itself, considered as a mechanical and biological object, responds to duty cycling, and reconciles findings that disagree in sign rather than merely in magnitude. Primary studies published between 2006 and 2026 were coded against a purpose-built parameterisation of non-steady operation comprising duty cycle, stop duration, cycle count, ramp rate, fluctuation amplitude and frequency, minimum-flux floor, idle-state fluid, flush protocol and buffering. Four membrane-side consequences are examined: irreversible compaction and creep recovery across repeated pressurisation; scaling induction time relative to residence time at peak supersaturation; biological regrowth during idle intervals; and permeate-quality transients on restart. Reported outcomes span a permeability loss exceeding fifty per cent after seven days of cycling and no measurable degradation after 1,568 start-stop cycles. Three variables reconcile most of that disagreement: idle-state chemistry, spontaneous osmotic backwash on depressurisation, and the partition between reversible compaction of the active layer and irreversible compaction of the support. No located study varies shutdown duration as a controlled independent variable against a biological endpoint on a membrane, and an experimental design closing that gap is specified.

ACCEPTED

03.09.26

Keywords: *Reverse osmosis; Intermittent operation; Membrane compaction; Biofouling; Photovoltaic desalination.*

CC BY

1. Introduction

Membrane-based systems have become the default technology for decentralised water supply where grid electricity and centralised treatment do not reach (Yin & Huang, 2026). For brackish groundwater in arid regions the dominant architecture is reverse osmosis driven by photovoltaic power, and Central Asia holds an early place in its record: a photovoltaic-powered reverse-osmosis pilot was

operated in Uzbekistan more than fifteen years ago (Aybar et al., 2010), preceded by solar direct-osmosis experiments in the same country (Khaydarov & Khaydarov, 2007). The engineering case for the architecture is settled. What is not settled is the condition of the membrane inside it: a photovoltaic system runs when the sun allows, stops at night, may stand idle for days, and delivers whatever flux the irradiance permits, not the flux at which the membrane was characterised.

Almost everything known about that membrane was measured under the opposite regime. The evidence base of membrane science rests on coupons of 5-45 cm² held at constant pressure and constant recovery, fed with synthetic solutions, over hours or days. This is not a shortcoming of individual studies but a constitutive property of the corpus. An audit conducted for this review of thirty-nine review articles published between 2019 and 2026 (1,090 typeset pages, roughly 800,000 words and 5,621 references in their combined bibliographies) found standardised testing protocols treated in none of them, long-term stability in three, and pilot- or field-scale evidence in seven. The mismatch between how membranes are characterised and how photovoltaic-driven systems make them operate is therefore not a gap in any one literature; it is a property of the literature as a whole.

Unsteady and cyclic desalination has recently been mapped at the level of process configurations, feed-channel hydrodynamics and data-driven control (Liang & Li, 2026), and batch-type configurations have been reviewed separately (Kim et al., 2025). The membrane's own response to that duty cycle, however, has not been substantively reviewed: irreversible compaction and creep recovery across repeated pressurisation-depressurisation cycles, rejection loss accumulated over cycles, and biological regrowth during idle intervals. Systematic reviews of solar-driven reverse osmosis continue to treat the membrane as a permeability coefficient and to address intermittency only as a generation-side problem (Almetwally et al., 2025). This review therefore takes the membrane - as a mechanical and biological object - rather than the process configuration as its unit of analysis.

A distinction is drawn throughout between *designed* cycling, in which the cycle is chosen and optimised as part of the process - batch, semi-batch and closed-circuit operation, and feed-flow reversal - and *imposed* cycling, in which the cycle is a disturbance dictated by the energy resource and must simply be survived. Existing treatments of fouling under cyclic operation address the former (Burlace 2022); the latter is the subject of this review. In photovoltaic-driven desalination the imposed cycle is diurnal and non-negotiable: the system stops every night, whatever the state of the membrane.

What that survival costs is not settled even in sign. Under seven days of daily cycling without a pre-shutdown flush, a brackish-water membrane retained less than half of its initial permeability, against more than seventy per cent when antiscalant dosing and a clean-water flush were applied (Freire-Gormaly & Bilton, 2019b). Under a comparable schedule observed by optical coherence tomography, intermittency protected rather than harmed: continuous operation lost 24% of flux where intermittent operation lost 8.9-10.4%, because the fouling layer collapsed from 21.2 μm to 7.5-8.4 μm at every shutdown (S. Lee et al., 2023). The variable separating these outcomes is what the membrane rests in, deionised water or feed, and where that has been varied directly it proves decisive (Yang et al., 2022). The full-scale record divides the same way: the longest intermittent record located, fourteen years at roughly nine hours per day, shows a permeability loss of about half, with specific energy consumption rising from 1.82 to 2.21 kWh m^{-3} (Ruiz-García 2020), while a seawater plant cycled hourly showed no structural degradation at autopsy after 1,568 start-stop events in four months (Carta et al., 2025).

This review organises the evidence around four membrane-side consequences of duty-cycled operation. The first is mechanical: polyamide composite membranes compact under load and recover incompletely, and the only located compaction study with an explicit cycle count reports the irrecoverable fraction growing cycle on cycle (Ding et al., 2024; Wu et al., 2025). The second is physicochemical: whether scaling occurs depends on how long the membrane resides at peak supersaturation relative to the nucleation induction time, a framing under which cycling has been found both protective (Warsinger et al.,

ISSN: 2181-3337 | SCIENTISTS.UZ

2018) and aggravating (T. Lee et al., 2019), a dispute treated here as the analytical core. The third is biological: regrowth during the idle interval, for which a surface endpoint has been measured under duty cycling (Freire-Gormaly 2019b), but in no located study with idle duration itself as the swept variable. The fourth is permeate quality on restart, where the literature conflates three phenomena that must be separated before results can be compared across studies: a recoverable hydrodynamic transient (Park et al., 2012), an unrecoverable loss of integrity accumulated over pressure cycles (Torii et al., 2019), and an instantaneous driving-force depression during low-power operation (Park et al., 2011).

The contribution intended here is not new data but reconciliation. Three variables already present in the primary literature, and assembled by no single source, account for most of the disagreement in sign: the chemistry of the idle state; the spontaneous osmotic backwash generated by depressurisation itself; and the partition of compaction into a reversible component in the active layer and an irreversible component in the support. A fourth, the scale and horizon of observation, accounts for much of the remainder. Section 2 states the search protocol and introduces a ten-field parameterisation of non-steady operation (Table 1), proposed as the reporting scheme the field currently lacks. Section 3 maps the evidence across the four consequences; Section 4 develops the reconciling variables; Section 5 ranks the resulting research priorities, the first of which is specified to the level of a full experimental design.

2. Method

This work is presented as an evidence map rather than as a systematic review. Bibliographic databases requiring institutional subscription were not accessible during the search, and the retrieval could not be re-executed under identical conditions; the protocol is therefore reported for transparency rather than as a reproducible procedure, and no PRISMA compliance is claimed. Records were located through Crossref, OpenAlex, Semantic Scholar, PubMed and publisher pages, supplemented by backward and forward citation tracking from four anchor studies (Freire-Gormaly & Bilton, 2018, 2019b; Ruiz-García & Nuez, 2020; Warsinger et al., 2018). Every bibliographic record reported here was confirmed against the publisher deposit; no publication year, volume or author list was inferred from an article identifier.

The corpus assembled under this protocol comprises sixty-nine bibliographic records. Eight are review articles, which delimit the surrounding territory without contributing evidence; four are industry standards and manufacturer technical bulletins, treated throughout as practitioner documentation rather than as peer-reviewed sources; the remaining fifty-seven are primary studies and constitute the evidence base mapped in Table 2. Eligibility required experimental observation of a reverse-osmosis or nanofiltration membrane under some form of non-steady operation: imposed start-stop duty cycling, resource-driven variable flux, repeated pressurisation, deliberately designed cyclic operation, or storage and stagnation between periods of service. One adjacent body of evidence was admitted deliberately. Studies of stagnation in drinking-water distribution and premise plumbing do not involve membranes, but they are the only systems located in this search in which idle duration is swept as a controlled independent variable against biological endpoints; they are used in Section 3.4 to define the shape of the response a membrane experiment should anticipate, not as evidence about membranes themselves.

Each primary study was coded against the ten descriptors of non-steady operation defined in Table 1: duty cycle, stop duration, cycle count, ramp rate, fluctuation amplitude and frequency, minimum-flux floor, idle-state fluid, flush protocol and buffering. No shared scheme of this kind was found in the literature, and its absence is consequential: blank cells in Table 2 were retained and never imputed, because what primary studies do not report is itself a finding. Figure 1 projects the coded corpus onto a matrix of non-steady mode against observation scale; the 43 studies shown are those whose observation scale could be verified, with modelling studies, re-analyses of existing datasets and the non-membrane stagnation studies excluded from the projection.

A terminological observation is itself a finding of this review. Querying "intermittent operation" alone recovers well under half of the relevant primary work, because the field is distributed across

ISSN: 2181-3337 | SCIENTISTS.UZ

vocabularies that do not cite one another. The productive alternative terms are "renewable energy powered membrane technology", "solar irradiance fluctuation", "osmotic backwash", "wave-driven pressure fluctuation", "transient membrane transport parameters", "salinity cycling", "compaction and relaxation", and "feed flow reversal". Searches confined to a single vocabulary will systematically under-represent the evidence base.

The fragmentation of vocabulary has an institutional counterpart on the side of standards. Standardisation in this field exists only on the feedwater side. A recent critical review of membrane autopsies cites eighteen ASTM standards, every one of them a method for analysing the feed - silt density index, modified fouling index, Langelier and Stiff-Davis saturation indices, chlorine, iron, silica and oxidation-reduction potential - and none a method for testing the membrane or the element (Philibert et al., 2024). The single ASTM method addressing element-level performance, D4194-23, prescribes measurement under standardised steady-state conditions and makes no provision for cyclic, intermittent or transient operation (ASTM International, 2023). The terminology standard for the field, D6161-19, defines no term for standby, lay-up, idle period, duty cycle, or cycle-count-based service life (ASTM International, 2019).

Table 1.

Proposed parameterisation scheme for non-steady reverse-osmosis operation

#	**Parameter**	**Unit / form of record**	**Example**	**Rationale**
1	Duty cycle	h operation / h idle per day	8/16; 9/15	Sets the ratio of filtration to stagnation
2	Stop duration	h or d of uninterrupted idleness	overnight; weekend; seasonal	Governs residence time at peak supersaturation relative to the nucleation induction time, and the interval available for biological regrowth
3	Cycle count	number of start-stop events per study	1,568 over 4 months	The only variable found to correlate with accumulated rejection loss
4	Ramp rate	kPa s^{-1} or LMH s^{-1} at start-up	soft start vs. step	Hydraulic shock and mechanical load on the element
5	Fluctuation amplitude	fraction of nominal flux	0.3-1.0	Amplitude of the diurnal irradiance excursion
6	Fluctuation frequency	h^{-1} or spectrum	cloud transients vs. diurnal cycle	Separates fast from slow disturbances
7	Minimum-flux floor	LMH below which the system idles	cut-in threshold	Below the floor: concentration polarisation without production
8	Idle-state fluid	contents of the element at rest	feed / permeate / DI / preservative	The decisive variable: determines the sign of the idle-period effect
9	Flush protocol	presence, timing and volume	permeate flush before shutdown	The best-evidenced mitigation in the corpus
10	Buffering	energy or water storage	permeate tank / battery / supercapacitor	Converts an energy-side problem into membrane protection

3. Results

3.1. The corpus at a glance

Table 2 maps the fifty-seven primary studies against the parameterisation of Table 1. Figure 1 projects the corpus onto a matrix of non-steady mode against observation scale, and its empty cells are findings in their own right. Three are consequential. Biological endpoints are absent above bench scale: no located study measures regrowth on an element or in a full plant with idle duration under experimental control. Compaction is absent under resource-driven flux: every measurement retrieved was made under stepped or programmed pressure, none under an irradiance-shaped profile. And the mechanical integrity of spiral-wound elements under repeated start-stop (hydraulic shock, telescoping, abrasion) has no located peer-reviewed literature, although it is a standing practitioner concern. The temporal profile of the corpus

ISSN: 2181-3337 | SCIENTISTS.UZ

(Figure 2) underlines how recently the field has begun to treat non-steadiness as a subject in its own right: half of all sixty-nine records (35) were published in 2022 or later. The four subsections that follow take the four membrane-side consequences in turn.

Table 2.

Evidence map of primary experimental studies under non-steady operation

Authors (Year)	Non-steady mode	Scale	Feed	Duration / cycles	Key finding
Imposed start-stop, coupon and bench					
Freire-Gormaly & Bilton (2019b)	Daily cycling, 8 h d^{-1}, 16 h idle	Bench + pilot element	Brackish groundwater	7 d	Antiscalant + flush retained >70% of initial permeability; <50% without flush; surface ATP quantified at autopsy
Zhang et al. (2019)	6, 12, 24 h d^{-1} schedules	Element (domestic)	Real tap water	90-180 d	Fouling-layer thickness grew with daily operating time; 6 h d^{-1} outperformed continuous; biofouling detectable at 7 d
Yang et al. (2022)	Two idle periods, fixed 3 h	Bench	$CaSO_4$ + colloidal silica	2 cycles	Benefit of intermittency governed by idle-state chemistry: DI recirculation restored flux, feed recirculation did not
S. Lee et al. (2023)	4/2 h and 8/16 h cycles; feed vs. DI at rest	Coupon (OCT in situ)	NaCl + humic acid	40 h over 5 d	Continuous lost 24% flux vs. 8.9-10.4% intermittent; fouling layer collapsed from 21.2 to 7.5-8.4 µm per shutdown
Dimitriou et al. (2025)	Steady vs. solar vs. cloudy-day profiles	Coupon	about 32 g L^{-1} NaCl	3 x 8 h d per scenario	Cloudy profile without rinse: −37% permeability, −18% rejection (combined compaction and fouling, not separated)
Sarker et al. (2025)	8 h d^{-1} cycling; end-of-day rinse	Bench	Gypsum-prone synthetic	6 d	End-of-day rinsing as a maintainability intervention
Imposed start-stop, full scale					
Ruiz-García & Nuez (2020)	About 9 h d^{-1} with pre-shutdown flush	Full plant, 416 m^3 d^{-1}	Real brackish groundwater	14 y	About 50% permeability loss; SEC 1.82 to 2.21 kWh m^{-3}; fouling acceleration from about day 500
Carta et al. (2025)	1 h on / 1 h off, continuous	Full plant, 100 m^3 d^{-1}	Real seawater	1,568 cycles / 4 mo	No structural degradation at autopsy; recovery improved by 0.12%
Kim et al. (2023)	Intermittent BWRO	Pilot	Brackish water	-	Biofouling under intermittent operation examined at pilot scale
Resource-driven variable flux					
Park et al. (2011)	Wind-driven fluctuating power incl. sub-threshold excursions	Pilot element	Synthetic brackish	h-scale runs	Flux and rejection track power non-linearly; rejection loss concentrated in low-power excursions
Park et al. (2012)	6 on-off cycles h^{-1}; stops 0.5-3 min	Prototype element	2,750-5,500 mg L^{-1} NaCl	1-h test periods	Restart salinity spike resolved against stop duration; sharper for shorter stops
Richards et al. (2015)	Irradiance fluctuation, 400-1,200 W m^{-2}	Bench PV-RO	Brackish	Event-scale	Irradiance steps of 100 W m^{-2} disrupt the polarisation layer via induced osmotic backwash
Cai et al. (2024)	Ramp rates 0.17-2 bar s^{-1}; up to 1,000 shut-downs	Bench crossflow	Synthetic	≤1,000 events	No significant deterioration at the highest ramp rate or cycle count; integrity loss only under forced permeate backpressure of 2-4 bar
Pressure cycling					
Torii et al. (2019)	Repeated pressurisation, household regime	Element + flat sheet	Virus-spiked water	10,000 cycles	About 4 $\log_{10}$ phage removal to 3,000-4,000 cycles, then collapse; replacement interval argued in cycles, not time
Sitterley et al. (2022)	Sinusoidal feed pressure, 500-900 psi	Pilot element	NaCl	About 1,770 h	7.4% irreversible permeability loss

ISSN: 2181-3337 | SCIENTISTS.UZ

Das et al. (2024)	Sinusoidal vs. rectified-sinusoidal waveforms	Element (SWRO)	Seawater	Multi-run	Waveform shape, not variability per se, governs damage; rectified waveform raised permeate salinity
Sitterley et al. (2025)	Trapezoidal ramps, ΔP 100-400 psi, 4-60 s	Pilot element	Dechlorinated tap + NaCl	28 dynamic conditions	A and B are not constants under transient pressure; transient parameters predict flux substantially better
Li (2026)	Dynamic and cyclic RO	Pilot (re-analysis of NREL datasets)	-	-	Counter-claim: permeability constant; apparent change is hysteresis of channel history
Designed cycling					
Warsinger et al. (2018)	Salinity cycling in batch RO	Bench + model	$CaSO_4$, $CaCO_3$, silica; real concentrates	Runs to 36 h	Residence at peak supersaturation 3-4 orders shorter than continuous RO; gypsum recovery limit rises from about 54 to above 90%
T. Lee et al. (2019)	Semi-batch vs. steady-state at matched recovery	Pilot element	Gypsum-supersaturated	Multi-run	Contrarian: semi-batch more scaling-prone; nucleation responds to peak, not time-averaged, supersaturation
Hosseinipour et al. (2023)	Free-piston batch RO	Element, 41 m^2	8 brackish compositions, LSI 1.7-2.6	>100 h / 96 tests	Zero scaling at calcite SI 2.6 without antiscalant; osmotic backwash 3.1-4.6 L per cycle as active cleaning
Tow et al. (2025)	Batch RO with flexible bladder	Pilot, to 5 $m^3\ d^{-1}$	Real concentrate, gypsum SI 0.63	885 cycles / 1 wk	No observable fouling at 82.6% recovery on supersaturated brine
Compaction and relaxation					
Ding et al. (2024)	Creep-recovery cycling, 8/16 h x 7	Coupon (DMA + EIS)	DI and model water	7 cycles; 10 loops	4.2% irrecoverable compaction per cycle, growing with each cycle
Wu et al. (2025)	TMP switching, 10-50 bar	Coupon	-	Stepped	Reversible compaction in the polyamide; irreversible in the support
Idle state and stagnation					
Ma et al. (2026)	Inter-cycle stagnation; 30-s flush at start/stop	Domestic 2-element system	Tap water	24 wk	Permeate TDS below 10 mg L^{-1} with flush vs. above 60 without; recovery 96.5 vs. 93.1% after 24 wk

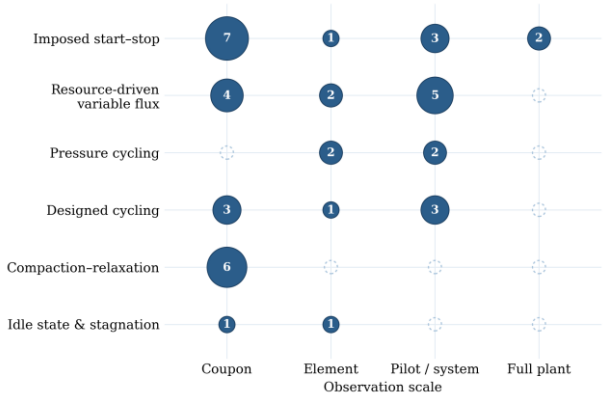


Figure 1. *Coverage of the primary experimental corpus by non-steady mode and observation scale.*

ISSN: 2181-3337 | SCIENTISTS.UZ

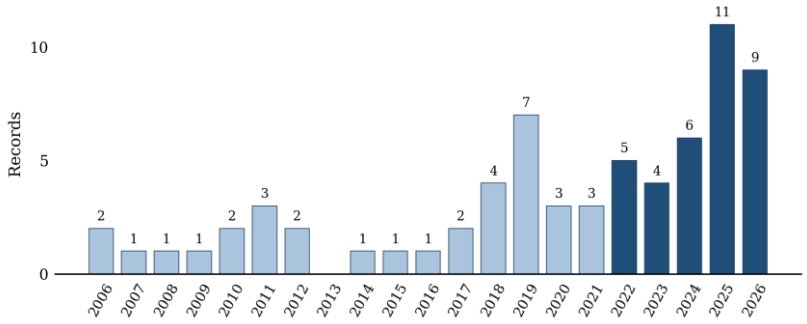


Figure 2. *Publication-year distribution of the corpus*

3.2. Compaction and viscoelastic recovery

The only located compaction study with an explicit cycle count is mechanical, not filtration-based. Under a duty cycle of 8 h load and 16 h recovery repeated seven times, with ten load-unload hysteresis loops and pressure steps to 330 psi, an NF270 membrane showed 15.0% initial compaction of which 10.8% recovered, leaving 4.2% irrecoverable per cycle, and the irrecoverable fraction grew cycle on cycle, which is fatigue in the ordinary materials-science sense of the word (Ding et al., 2024). The RO membrane in the same study compacted 20.9% at 200 psi, and the ratio of creep to instantaneous deformation rose from 8% to 94% across the pressure steps: at operating pressures, most of what the membrane does under load is time-dependent.

Where that deformation resides has been resolved. Compaction scales with transmembrane pressure (up to 30% at 50 bar against under 10% at 10 bar), and switching between high and low pressure does not appreciably change its extent, because the highly cross-linked polyamide recovers on depressurisation while compaction of the polysulfone support is largely irreversible (Wu et al., 2025). Positron annihilation lifetime spectroscopy independently locates the irreversible component outside the selective layer: at 150 bar the support loses about 60% of cross-sectional thickness and up to 95% of surface porosity while the selective layer does not irreversibly compact (Davenport et al., 2020). The polyamide itself is not inert, however: it densifies under load and relaxes only partially, and higher cross-linking buys smaller compaction and better recovery at the price of initial permeability (Wu et al., 2024), a materials lever directly relevant to membranes destined for cyclic duty.

At element scale the phenomenon persists. Some 1,770 h of sinusoidal feed-pressure cycling between 500 and 900 psi left a 7.4% irreversible permeability loss (Sitterley et al., 2022), and compaction under cyclic batch loading carries a measurable energy cost (Patel et al., 2024). Nor is the mechanics confined to the polymer: a gel foulant layer itself exhibits compaction-relaxation hysteresis with distinct time constants for compression and swelling, and oscillating pressure can raise its permeability relative to static load (Epstein & Ramon, 2026), and biofilms compact and relax in the same manner (Valladares Linares et al., 2016). One coupon study emulating photovoltaic profiles reports a 37% permeability loss over three cloudy-day cycles without an end-of-day rinse; the authors attribute the degradation to compaction and fouling jointly and do not separate the two, so the figure is evidence of the combined mechanism only (Dimitriou et al., 2025).

3.3. Scaling: induction time against residence time

A shutdown is, physically, a period of residence at the highest supersaturation the system reaches: permeation stops, the concentration-polarisation layer and the concentrated brine remain, and whether crystals form is then a race against the nucleation induction time. The framing originates in deliberately cyclic operation. Scaling can be prevented by "zeroing" the elapsed nucleation time: interrupting supersaturation before induction completes, demonstrated for calcium sulfate (Pomerantz et al., 2006) and building on the concept of periodic feed-flow reversal introduced by the same group (Gilron et al., 2006). The principle has since been instrumented: flow reversal triggered by ex-situ optical detection of incipient nucleation controlled gypsum scaling in a brackish-water pilot (Uchymiak et al., 2009), and forward-

ISSN: 2181-3337 | SCIENTISTS.UZ

reverse cycles switched by ultrasonic detection of deposit onset avoided the flux decline of continuous forward flow at bench scale (Lu et al., 2012). In these systems the cycle is timed by the chemistry, through a sensor or a schedule set against the induction time. A photovoltaic system executes the same interruption with the timing surrendered to the resource: the sun, not the saturation state, decides when permeation stops.

The batch literature shows how protective the interruption can be when residence times are short. In batch reverse osmosis the residence time at peak supersaturation is three to four orders of magnitude shorter than in continuous operation, so the induction time is never exceeded, and the gypsum-limited recovery ceiling rises from about 54% to above 90% (Warsinger et al., 2018). The prediction has survived severe field tests: 885 cycles in a single week at 82.6% recovery on a real, gypsum-supersaturated concentrate (saturation index 0.63) produced no observable fouling (Tow et al., 2025), and a free-piston batch system desalinating eight brackish groundwater compositions showed zero scaling at calcite saturation indices up to 2.6 without antiscalant, with the depressurisation-driven osmotic backwash of 3.1-4.6 L per cycle identified as an active cleaning mechanism (Hosseinipour et al., 2023). Induction times themselves are becoming predictable, through machine learning grounded in Smoluchowski theory (Abdelkawi et al., 2025) and through a survival-analysis framework for dynamically concentrating systems (Abdelkawi et al., 2026).

The contrarian result defines the boundary of the protection. At matched recovery, semi-batch operation proved more scaling-prone than steady-state reverse osmosis, in both crystal growth rate and scaled area, because nucleation responds to the peak supersaturation the cycle repeatedly visits, not to its time average (T. Lee et al., 2019). Cycling therefore protects only while the excursion above saturation stays shorter than induction; a cycle that repeatedly samples high peak supersaturation can be worse than the steady state it replaces. Under imposed cycling the corpus is thinner but consistent with the frame, much of it produced on a rig purpose-built to impose intermittency (Freire-Gormaly & Bilton, 2017): real-time imaging resolves scale formation on the membrane surface under intermittent operation (Sarker & Bilton, 2021), a pre-shutdown clean-water flush with antiscalant preserved more than 70% of initial permeability where its absence left less than 50% (Freire-Gormaly & Bilton, 2019b), and end-of-day rinsing has been advanced as a maintainability intervention for photovoltaic systems (Sarker et al., 2025).

3.4. Biological regrowth during idle intervals

What has been measured on membranes is quickly stated. Surface adenosine triphosphate was quantified at autopsy after seven days of duty cycling, with the shutdown interval fixed at 16 h by the 8 h d^{-1} schedule (Freire-Gormaly & Bilton, 2019b). Daily schedules of 6, 12 and 24 h have been compared over 90-180 days on real tap water, with biofouling detectable by day 7, fouling-layer thickness growing with daily operating time, and the 6 h d^{-1} schedule outperforming continuous operation (Zhang et al., 2019), but the comparison varies operating time and idle time together. The one study that varies the resting state directly holds idle duration fixed at 3 h and makes no biological measurement at all (Yang et al., 2022). Biofouling under intermittent operation has been examined at pilot scale in a brackish-water system (Kim et al., 2023). The steady-state biofouling literature, by contrast, is mature (Hoek et al., 2022), which is precisely what makes the idle interval the untreated variable.

Biological endpoints have been measured on reverse-osmosis membranes under duty-cycled operation - surface adenosine triphosphate in the case of Freire-Gormaly and Bilton (2019b) - but in every located study the shutdown interval is fixed by the application's diurnal or demand cycle rather than swept as a controlled independent variable. What is varied instead is the state of the membrane at rest: lay-up chemistry (Yang et al., 2022) or end-of-shift rinsing (Sarker et al., 2025). Where idle duration has been swept against biological endpoints, the systems are not membranes but drinking-water distribution and premise plumbing, in which the response proves markedly non-linear: thresholds are reported at two and four hours (Ren et al., 2025), and attenuation rates are resolvable per hour of stagnation (Elliott et al.,

ISSN: 2181-3337 | SCIENTISTS.UZ

2011). The coupling between idle duration and biological regrowth on a polyamide membrane is therefore not quantified, even where biofouling under intermittent operation has been examined at pilot scale (Kim et al., 2023).

The non-membrane evidence indicates what a membrane experiment should expect. With stagnation swept from 0.25 to 10 h, microbial diversity falls and *Legionella pneumophila* rises significantly beyond thresholds at 2 and 4 h, driven by accelerating chlorine decay (Ren et al., 2025). Overnight stagnation alone raises cell counts two- to three-fold and adenosine triphosphate two- to eighteen-fold (Lautenschlager et al., 2010); after roughly six days, counts climb from 10^3 to 7.8×10^5 cells mL^{-1} (Ling et al., 2018); intervals up to 168 h have been resolved against total and intact cell counts across seasons (Zlatanović et al., 2017). Idle time is not uniformly hostile: in household slow sand filters, virus attenuation proceeds at up to 0.061 log_{10} per hour of idle time, and the effect vanishes when microbial activity is suppressed, a microbially mediated benefit of standing still (Elliott et al., 2011). In these systems idle duration is the controlled variable and the response is non-linear with thresholds at the scale of hours, in the diurnal range of a photovoltaic plant; Figure 3 places the located studies on this axis.

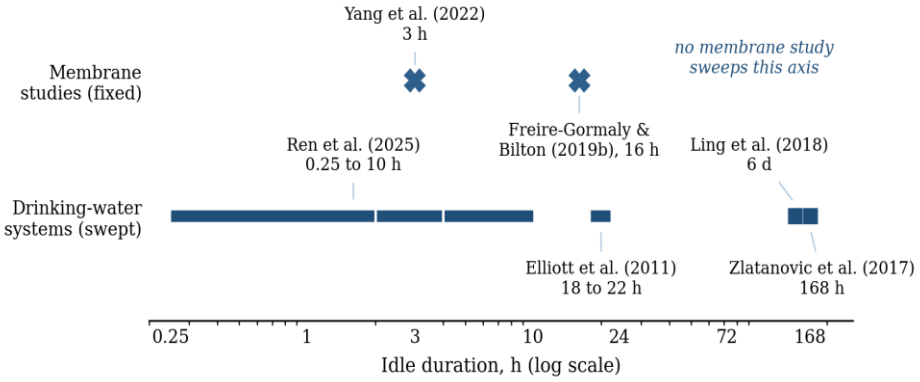


Figure 3. *Idle duration as an experimental variable: ranges swept in drinking-water systems against fixed values in located membrane studies.*

3.5. Permeate quality on restart

The literature conflates three distinct phenomena that this review separates. The first is the transient conductivity excursion during and immediately after a restart, which is hydrodynamic and recoverable, and which has been resolved against shutdown duration only once (Park et al., 2012). The second is the cumulative loss of rejection with cycle count, which is a matter of membrane integrity and is not recoverable (Torii et al., 2019). The third is the depression of rejection during low-power operation, which is a driving-force effect and is instantaneous (Park et al., 2011). No prior source distinguishes them, and conclusions drawn about "permeate quality under intermittent operation" are not comparable across studies until they are separated.

The single resolution of the first phenomenon against stop duration yielded a counter-intuitive result: across six on-off cycles per hour, the permeate salinity spike on restart was sharper after stops of 0.5-1 min than after stops of 1-3 min (Park et al., 2012). The transient also responds to mitigation over long horizons: in a domestic two-element system cycled for 24 weeks, a 30-s flush at start and stop held permeate total dissolved solids below 10 mg L^{-1} against above 60 mg L^{-1} in the unflushed control, and recovery after 24 weeks stood at 96.5% against 93.1%; stagnation accelerates long-term degradation as well as the restart excursion (Ma et al., 2026). The second phenomenon has a cycle count attached: over 10,000 pressurisation cycles emulating household duty, removal of the φX-174 bacteriophage held near 4 log_{10} for the first 3,000-4,000 cycles and then collapsed, with even *Escherichia coli* penetrating by 10,000; the damage localised near the membrane surface, and the authors argue that replacement intervals should be set in cycles, not calendar time (Torii et al., 2019). Intermittency has since been examined against

ISSN: 2181-3337 | SCIENTISTS.UZ

membrane integrity directly: across feed-pressure ramp rates of 0.17-2 bar s^{-1} and up to 1,000 shut-down events, no significant performance deterioration was observed, and integrity loss appeared only when a permeate backpressure of 2-4 bar was applied to force the backwash (Cai et al., 2024). For the third phenomenon, the shape of the disturbance matters as much as its size: rejection loss under wind-driven power concentrates in low-power excursions (Park et al., 2011), and at element scale a rectified-sinusoidal waveform raised permeate salinity where a smooth sinusoid of equal variability behaved like the steady-state reference (Das et al., 2024). Whether any of this reflects a change in the membrane's own transport properties is disputed in print: transient, pressure-dependent water and salt permeability coefficients predict flux substantially better than constant ones (Sitterley et al., 2025), against the counter-claim that permeability is constant and the apparent change is hysteresis of the flow channel's history (Li, 2026). Null results bound the problem from above: unsteady power did not measurably affect product water quality in long-term field operation (Schäfer et al., 2018), solute rejection proved resilient across membranes under irradiance fluctuation (Boussouga et al., 2021) as under battery-less photovoltaic operation on real brackish groundwater (Richards et al., 2008), resilient operating windows have been mapped for photovoltaic-membrane systems under transient solar conditions (Ogunniyi & Richards, 2026), and the hourly-cycled seawater plant improved its recovery by 0.12% over 1,568 cycles (Carta et al., 2025).

3.6. Five axes of disagreement

Read together, the corpus disagrees in sign along five axes, collected in Table 3: bench-scale harm against bench-scale protection; full-scale degradation over fourteen years against a full-scale null over four months; scaling suppressed by cycling against scaling aggravated by it; rejection collapse with cycle count against unchanged product quality; and transport properties that vary under transient pressure against a constant-permeability counter-claim. None of these is a contradiction to be adjudicated by majority vote. Each is resolved, or in one case delimited, by a variable the primary studies already contain, and that resolution is the subject of the following section.

Table 3.

Disagreements in sign across the evidence base and their reconciling variables

Axis	Study A: finding (sign)	Study B: finding (sign)	Reconciling variable
1. Coupon and bench scale	Freire-Gormaly & Bilton (2019b): <50% of initial permeability after 7 d of cycling without a pre-shutdown flush (harmful)	S. Lee et al. (2023): 24% flux loss under continuous operation vs. 8.9-10.4% under intermittent; fouling layer collapses from 21.2 to 7.5-8.4 μm per shutdown (protective)	Idle-state chemistry: DI vs. feed water (Yang et al., 2022)
2. Full scale, different horizons	Carta et al. (2025): no structural degradation after 1,568 start-stop cycles in 4 months; recovery improved by 0.12% (neutral)	Ruiz-García & Nuez (2020): about 50% permeability loss over 14 years at about 9 h d^{-1}; SEC 1.82 to 2.21 kWh m^{-3} (harmful)	Observation horizon: fouling acceleration begins near day 500, after the four-month window
3. Scaling under cycling	Warsinger et al. (2018); Tow et al. (2025): residence at peak supersaturation 3-4 orders of magnitude shorter than continuous RO; 885 cycles at gypsum SI 0.63 with no observable fouling (protective)	T. Lee et al. (2019): semi-batch RO more scaling-prone than steady-state at matched recovery (harmful)	Nucleation responds to peak, not time-averaged, supersaturation
4. Permeate quality	Torii et al. (2019): rejection collapse after 3,000-4,000 pressure cycles (harmful)	Schäfer et al. (2018); Carta et al. (2025): unsteady power did not measurably affect water quality; recovery even improved (neutral)	Three conflated phenomena: restart transient, integrity loss, driving-force depression (Section 3.5)
5. Transport properties vs.	Sitterley et al. (2025): A and B are not constants under transient	Li (2026): permeability constant; apparent change is hysteresis of	Interpretive framework applied to

ISSN: 2181-3337 | SCIENTISTS.UZ

channel history	pressure; transient parameters predict flux substantially better (properties change)	channel history (properties constant)	the same pilot-scale data; unresolved dispute in print

4. Discussion

None of the five axes of Table 3 is settled by weighing studies against one another. Each disagreement dissolves once a variable already present in the primary data, but assembled by no single source, is made explicit. Four such variables organise this section, and Figure 4 locates each of them on the anatomy of a single start-stop event; two closing subsections address a terminological collision with the nearest prior review and the relation between the scholarly and the practitioner literatures.

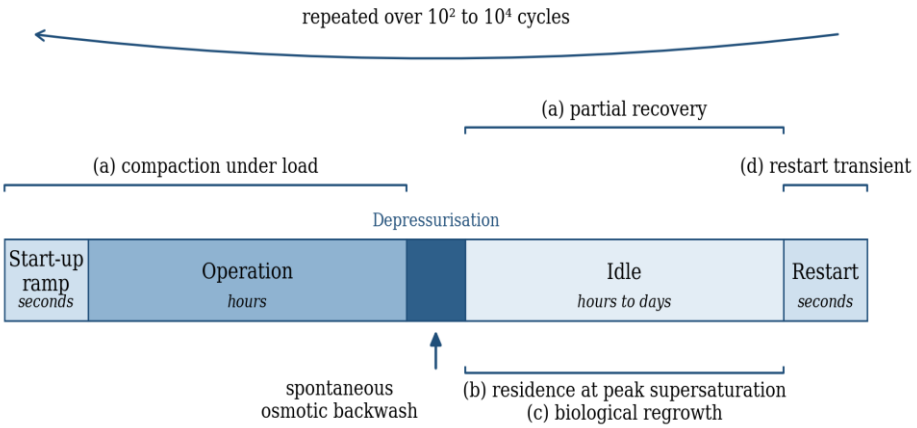


Figure 4. *Phases of a start-stop event and the membrane-side consequences (a)-(d). Time axis not to scale.*

4.1. The chemistry of the idle state

The bench-scale contradiction of axis 1 is not a contradiction but two different experiments. In the study that found harm, the membrane rested in the scaling-prone feed it had been concentrating all day (Freire-Gormaly & Bilton, 2019b); in the study that found protection, every shutdown collapsed the fouling layer and the resting fluid differed (S. Lee et al., 2023). The one study that varies the resting state directly, at fixed idle duration, finds the benefit of intermittency governed by exactly this: deionised-water recirculation restored flux, feed recirculation did not (Yang et al., 2022). The same gradient is visible within a single experiment: intermittent operation resting in deionised water lost 8.9% of flux against 10.4% resting in feed (S. Lee et al., 2023). The practical corollary inverts the usual reading of the pre-shutdown flush. It is not housekeeping; it is the variable that sets the sign of the idle-period effect, which is why its presence or absence separates retention of more than 70% of initial permeability from less than 50% (Freire-Gormaly & Bilton, 2019b; Figure 5) and why end-of-day rinsing is the intervention proposed for photovoltaic systems specifically (Sarker et al., 2025), the measured penalty having already been carried into design guidance for such systems (Freire-Gormaly & Bilton, 2019a). What none of these studies measures is biology at rest: idle-state chemistry resolves the mineral and colloidal side of axis 1 and leaves its biological side inside the gap of Section 3.4.

ISSN: 2181-3337 | SCIENTISTS.UZ

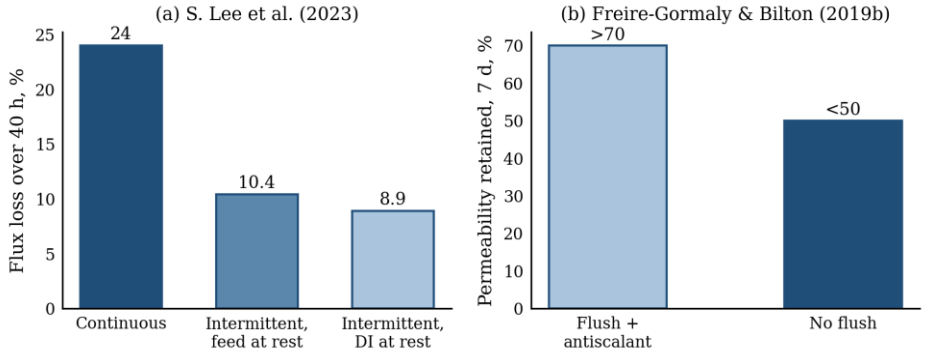


Figure 5. *Idle-state fluid and pre-shutdown flushing set the sign of the idle-period effect: (a) flux loss by resting fluid; (b) permeability retained with and without a pre-shutdown flush.*

4.2. Spontaneous osmotic backwash

The second variable explains why stopping can clean. When permeation ceases and pressure falls, the osmotic gradient across the membrane briefly reverses the water flux, lifting deposited material off the surface. The mechanism was identified under fluctuating irradiance, where steps as small as 100 W m^{-2} disrupt the concentration-polarisation layer through naturally induced osmotic backwash (Richards et al., 2015), and has since been resolved into its direct and spontaneous forms (Cai & Schäfer, 2020), characterised against mineral scaling (Cai et al., 2021), and traced mechanistically to the adhesive energetics between membrane and organic matter (Cai et al., 2022), with its bearing on membrane integrity under intermittency examined in the same series (Cai et al., 2024). In batch operation the depressurisation-driven backwash is measured in litres per cycle and identified as an active cleaning mechanism (Hosseinipour et al., 2023). The synthesis none of these sources draws is that every shutdown of a photovoltaic system performs, without design effort, what batch configurations engineer deliberately. The first two variables then act in sequence: the backwash operates over the seconds of depressurisation, the idle-state chemistry over the hours that follow; a shutdown that begins with a cleaning event can still end in a scaled or colonised membrane if the element is left standing in concentrate.

4.3. The partition of compaction and a hypothesis

The third variable reconciles short and long observations of the same mechanics. Compaction partitions into a reversible component in the polyamide active layer and a largely irreversible component in the polysulfone support (Wu et al., 2025; Davenport et al., 2020), and the irrecoverable fraction accumulates cycle on cycle (Ding et al., 2024). A single depressurisation therefore shows little, because the reversible component masks the irreversible one, while a multi-day cycle accumulates damage; experiments differing only in horizon will disagree in sign with no error on either side.

No study located in this review measured compaction under resource-driven variable flux, and no study of photovoltaic-powered operation measured compaction. The proposition advanced here - that reversible compaction and its incomplete relaxation account for part of the flux hysteresis currently attributed to fouling in the photovoltaic reverse-osmosis literature - is therefore a hypothesis this review advances rather than a finding it reports, and it is labelled as such throughout.

Two pieces of arithmetic, offered as such and not as evidence, mark the size of the open question (Figure 6). A batch pilot executed 885 cycles in a single week (Tow et al., 2025); the only explicit fatigue measurement reports 4.2% irrecoverable compaction per cycle under an 8/16 h duty (Ding et al., 2024). These numbers do not meet: the loading profiles differ by orders of magnitude (seconds-scale depressurisation against sixteen-hour holds), and no located study bridges them, which is itself an argument for reporting ramp rate and duty cycle as Table 1 prescribes. The second: 1,568 start-stop events in four months produced no measurable change at full scale (Carta et al., 2025). Whether coupon-scale fatigue fails to express at element scale, or expresses on horizons longer than four months, is precisely what the corpus cannot yet say.

ISSN: 2181-3337 | SCIENTISTS.UZ

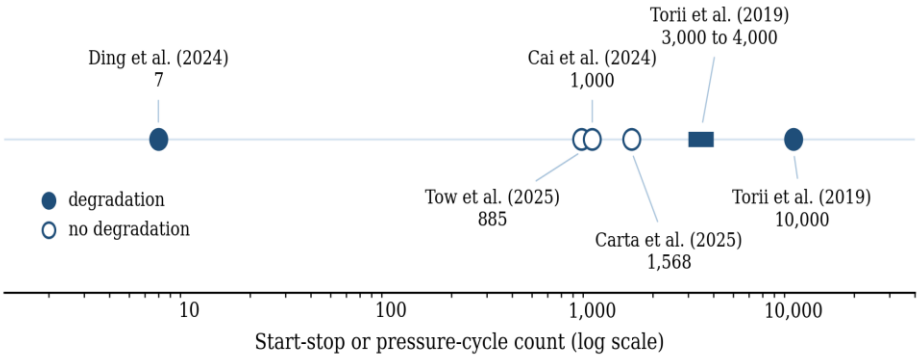


Figure 6. *Reported start-stop and pressure-cycle counts with associated outcomes. Cycle definitions differ between studies.*

4.4. Scale and horizon of observation

The fourth variable is the observation itself. Axis 2 sets a four-month full-scale null (Carta et al., 2025) against a 50% permeability loss over fourteen years (Ruiz-García & Nuez, 2020). The two are consistent with a single degradation curve, since fouling acceleration in the fourteen-year record begins near day 500, beyond the entire window of the four-month study; but consistency is not demonstration: no located data resolve the shape of that curve between four months and fourteen years, and the claim is left as the weaker one. Axis 5 is delimited rather than resolved. Transient, pressure-dependent transport coefficients predict flux substantially better than constants at element scale (Sitterley et al., 2025); the counter-claim holds permeability constant and attributes the apparent variation to the hysteresis of the flow channel's history (Li, 2026). The claims are not symmetric: one estimates parameters from element-scale transients, the other relocates the phenomenon upstream of the membrane. Deciding between them requires an experiment that separates membrane from channel, which is exactly the separation the reporting scheme of Table 1 makes expressible. The dispute is in print, current, and open.

4.5. A terminological collision

A terminological distinction should be noted. The "cycle-to-cycle salt accumulation" identified as a research gap by Liang and Li (2026) refers to salt accumulating in the recirculating brine between cycles, a mass-balance and flushing phenomenon at the process level. It is distinct from the accumulated loss of salt rejection by the membrane material that is examined here, which is a property of the active layer, not of the fluid inventory.

The same review's reported membrane-life extension exceeding 100% is a result of machine-learning-based control demonstrated at industrial scale, not a materials-level analysis, and does not bear on the membrane-side questions treated here.

4.6. The practitioner literature and its missing counterpart

A large practitioner literature governs the idle state, and it has no scholarly counterpart. Manufacturers prescribe preservation for any shutdown exceeding forty-eight hours, specify one to one and a half per cent sodium metabisulfite, cap pressurisation and depressurisation at ten pounds per square inch per second, and state plainly that elements allowed to dry after service may lose water permeability irreversibly. None of these thresholds is derived from a published experiment. The asymmetry is illustrated by the peer-reviewed literature itself: a study of preservation chemistry published in this field's principal materials journal cites a manufacturer's technical service bulletin as the source of its chemistry (Tu et al., 2014).

The peer-reviewed counterpart is confined to a handful of studies: a comparative assessment of non-oxidising biocides against sodium metabisulfite (Majamaa et al., 2011) and the preservation-chemistry study already named, which found permeability rising 10-20% after storage while boron and sodium rejection losses exceeded the permeability change in magnitude (Tu et al., 2014). A recent review of

ISSN: 2181-3337 | SCIENTISTS.UZ

membrane drying addresses preservation of membranes as stored artefacts, adjacent to but distinct from the repeated wet-idle cycling of membranes in service (Van Buggenhout et al., 2025). The nearest located test touches one threshold from below: at bench scale, feed-pressure ramp rates up to 2 bar s^{-1}, nearly three times the 0.7 bar s^{-1} practitioner cap (Hydranautics, 2019), produced no membrane damage (Cai et al., 2024); whether the cap is conservative or protective at spiral-wound element scale is exactly the untested proposition. Every quantitative threshold in service today, from the forty-eight-hour rule (DuPont Water Solutions, 2026) to the ramp-rate cap and the biocide concentrations, still awaits its first published experiment at the scale it governs.

5. Conclusion and Implications

Five research priorities follow, in order of leverage.

First, no located study isolates idle duration as the controlled independent variable for biological regrowth on a reverse-osmosis membrane; the shutdown interval is everywhere fixed by the application while the resting state is varied instead. Closing this gap requires a factorial design in which idle duration is the primary independent variable, swept across at least four levels spanning the diurnal range from one hour to seventy-two hours, crossed with idle-state fluid (feed, permeate, deionised water) and with feed biological loading. Endpoints must be biological - adenosine triphosphate, quantitative PCR of total and viable cells, and extracellular polymeric substance quantification - and must be measured on the membrane surface rather than in the bulk. The design should anticipate a non-linear rather than a monotonic response, since threshold behaviour at intervals of two to four hours has been reported in analogous stagnant systems (Ren et al., 2025).

Second, compaction hysteresis under a photovoltaic-representative duty cycle remains unmeasured in the retrieved corpus; until one does, the hypothesis of Section 4.3, that part of the flux hysteresis now attributed to fouling is viscoelastic, remains open in both directions.

Third, no peer-reviewed study was located on hydraulic transients, water hammer, or mechanical damage at the spiral-wound element scale under start-stop operation, although practitioner documentation caps ramp rates numerically; the distance between a prescribed threshold and a published experiment is short here, and closable.

Fourth, the field has no shared reporting standard for non-steady operation, and the blank cells of Table 2 price that absence; the ten-field scheme of Table 1 is proposed as that standard; the most recent accelerated-ageing protocol for spiral-wound elements takes accumulated exposure, not the number of transitions, as its dose variable (Alkhouzaam & Khraisheh, 2026), which is exactly the quantity the scheme adds.

Fifth, the retrieved corpus contains no field data from the gypsum-prone brackish groundwaters of Central Asia, although the region hosts some of the earliest photovoltaic desalination work (Aybar et al., 2010; Khaydarov & Khaydarov, 2007) and the induction-time framework of Section 3.3 is directly computable for its water compositions. That field campaign is the natural next work of the present authors.

Acknowledgment

This work was supported by grant FL-9024093713 from the Physical-technical Institute named after S.A. Azimov, Academy of Sciences of the Republic of Uzbekistan.

REFERENCES

1. Abdelkawi, A. A., Lindsey, J. L., & Wright, N. C. (2025). Prediction of gypsum induction time to inform scaling kinetics using machine learning and Smoluchowski theory. *Desalination, 616*, Article 119288. https://doi.org/10.1016/j.desal.2025.119288
2. Abdelkawi, A. A., Lindsey, J. L., & Wright, N. C. (2026). A survival analysis framework for predicting gypsum scaling risk in dynamically concentrating desalination systems. *Water Research, 304*, Article 126345. https://doi.org/10.1016/j.watres.2026.126345

ISSN: 2181-3337 | SCIENTISTS.UZ

3. Alkhouzaam, A., & Khraisheh, M. (2026). Field-realistic accelerated aging protocol for spiral-wound reverse osmosis membranes: Multi-scale diagnostics and end-of-life criteria. *Desalination, 628*, Article 120071. https://doi.org/10.1016/j.desal.2026.120071
4. Almetwally, E. M., Elazab, M., Kabeel, A., Yasser, Y., & Elgebaly, A. (2025). Solar powered reverse osmosis desalination: A systematic review of technologies, integration strategies and challenges. *Desalination, 615*, Article 119228. https://doi.org/10.1016/j.desal.2025.119228
5. ASTM International. (2019). *Standard terminology used for microfiltration, ultrafiltration, nanofiltration, and reverse osmosis membrane processes* (ASTM D6161-19). ASTM International.
6. ASTM International. (2023). *Standard test methods for operating characteristics of reverse osmosis and nanofiltration devices* (ASTM D4194-23). ASTM International. https://doi.org/10.1520/D4194-23
7. Aybar, H. S., Akhatov, J. S., Avezova, N. R., & Halimov, A. S. (2010). Solar powered RO desalination: Investigations on pilot project of PV powered RO desalination system. *Applied Solar Energy, 46*(4), 275-284. https://doi.org/10.3103/S0003701X10040080
8. Boussouga, Y.-A., Richards, B. S., & Schäfer, A. I. (2021). Renewable energy powered membrane technology: System resilience under solar irradiance fluctuations during the treatment of fluoride-rich natural waters by different nanofiltration/reverse osmosis membranes. *Journal of Membrane Science, 617*, 118452. https://doi.org/10.1016/j.memsci.2020.118452
9. Burlace, L., & Davies, P. (2022). Fouling and fouling mitigation in batch reverse osmosis: Review and outlook. *Desalination and Water Treatment, 249*, 1-22. https://doi.org/10.5004/dwt.2022.28103
10. Cai, Y.-H., Boussouga, Y.-A., & Schäfer, A. I. (2024). Renewable energy powered membrane technology: Impact of intermittency on membrane integrity. *Desalination, 580*, 117504. https://doi.org/10.1016/j.desal.2024.117504
11. Cai, Y.-H., Burkhardt, C. J., & Schäfer, A. I. (2021). Renewable energy powered membrane technology: Impact of osmotic backwash on scaling during solar irradiance fluctuation. *Journal of Membrane Science, 619*, 118799. https://doi.org/10.1016/j.memsci.2020.118799
12. Cai, Y.-H., Gopalakrishnan, A., Deshmukh, K. P., & Schäfer, A. I. (2022). Renewable energy powered membrane technology: Implications of adhesive interaction between membrane and organic matter on spontaneous osmotic backwash cleaning. *Water Research, 221*, 118752. https://doi.org/10.1016/j.watres.2022.118752
13. Cai, Y.-H., & Schäfer, A. I. (2020). Renewable energy powered membrane technology: Impact of solar irradiance fluctuation on direct osmotic backwash. *Journal of Membrane Science, 598*, 117666. https://doi.org/10.1016/j.memsci.2019.117666
14. Carta, J. A., Cabrera, P., Melián-Martel, N., & Arenas-Urrea, S. (2025). Experimental investigation of the effect of intermittent operation on membranes in wind-powered SWRO plants, focusing on frequent start-stop scenarios. *Energy Conversion and Management: X, 25*, Article 100848. https://doi.org/10.1016/j.ecmx.2024.100848
15. Das, T. K., Folley, M., Lamont-Kane, P., & Frost, C. (2024). Performance of a SWRO membrane under variable flow conditions arising from wave powered desalination. *Desalination, 571*, Article 117069. https://doi.org/10.1016/j.desal.2023.117069
16. Davenport, D. M., Ritt, C. L., Verbeke, R., Dickmann, M., Egger, W., Vankelecom, I. F. J., & Elimelech, M. (2020). Thin film composite membrane compaction in high-pressure reverse osmosis. *Journal of Membrane Science, 610*, Article 118268. https://doi.org/10.1016/j.memsci.2020.118268
17. Dimitriou, E., Loukatos, D., Arvanitis, K. G., & Papadakis, G. (2025). Experimental evaluation of the performance of a flat sheet reverse osmosis membrane under variable and intermittent operation emulating a photovoltaic-driven desalination system. *Water, 17*(24), Article 3576. https://doi.org/10.3390/w17243576

ISSN: 2181-3337 | SCIENTISTS.UZ

18. Ding, W., Ma, K., & Childress, A. E. (2024). Compaction of pressure-driven water treatment membranes: Real-time quantification and analysis. *Environmental Science & Technology, 58*(41), 18404-18413. https://doi.org/10.1021/acs.est.4c05865
19. DuPont Water Solutions. (2026). *Reverse osmosis - Handling, preservation and storage* (Technical manual excerpt, Form No. 45-D03716-en, Rev. 11). DuPont de Nemours.
20. Elliott, M. A., DiGiano, F. A., & Sobsey, M. D. (2011). Virus attenuation by microbial mechanisms during the idle time of a household slow sand filter. *Water Research, 45*(14), 4092-4102. https://doi.org/10.1016/j.watres.2011.05.008
21. Epstein, J. A., & Ramon, G. Z. (2026). Characterizing the permeability of a foulant layer under a transient applied pressure. *Journal of Membrane Science, 738*, Article 124683. https://doi.org/10.1016/j.memsci.2025.124683
22. Freire-Gormaly, M., & Bilton, A. (2017). An experimental system for characterization of membrane fouling of solar photovoltaic reverse osmosis systems under intermittent operation. *Desalination and Water Treatment, 73*, 54-63. https://doi.org/10.5004/dwt.2017.20391
23. Freire-Gormaly, M., & Bilton, A. M. (2018). Experimental quantification of the effect of intermittent operation on membrane performance of solar powered reverse osmosis desalination systems. *Desalination, 435*, 188-197. https://doi.org/10.1016/j.desal.2017.09.013
24. Freire-Gormaly, M., & Bilton, A. M. (2019a). Design of photovoltaic powered reverse osmosis desalination systems considering membrane fouling caused by intermittent operation. *Renewable Energy, 135*, 108-121. https://doi.org/10.1016/j.renene.2018.11.065
25. Freire-Gormaly, M., & Bilton, A. M. (2019b). Impact of intermittent operation on reverse osmosis membrane fouling for brackish groundwater desalination systems. *Journal of Membrane Science, 583*, 220-230. https://doi.org/10.1016/j.memsci.2019.04.010
26. Gilron, J., Waisman, M., Daltrophe, N., Pomerantz, N., Milman, M., Ladizhansky, I., & Korin, E. (2006). Prevention of precipitation fouling in NF/RO by reverse flow operation. *Desalination, 199*(1-3), 29-30. https://doi.org/10.1016/j.desal.2006.03.136
27. Hoek, E. M. V., Weigand, T. M., & Edalat, A. (2022). Reverse osmosis membrane biofouling: Causes, consequences and countermeasures. *npj Clean Water, 5*, Article 45. https://doi.org/10.1038/s41545-022-00183-0
28. Hosseinipour, E., Harris, E., El Nazer, H. A., Mohamed, Y. M. A., & Davies, P. A. (2023). Desalination by batch reverse osmosis (RO) of brackish groundwater containing sparingly soluble salts. *Desalination, 566*, Article 116875. https://doi.org/10.1016/j.desal.2023.116875
29. Hydranautics. (2019). *Membrane start-up, shutdown, and preservative flushing guidelines* (Technical Service Bulletin TSB118.16). Nitto Group. https://membranes.com/wp-content/uploads/Documents/TSB/TSB118.pdf
30. Khaydarov, R. A., & Khaydarov, R. R. (2007). Solar powered direct osmosis desalination. *Desalination, 217*(1-3), 225-232. https://doi.org/10.1016/j.desal.2007.03.004
31. Kim, G., Song, Y., Hwang, T.-M., Park, Y.-G., Davies, P. A., & Park, K. (2025). Practical implementation and challenges of current batch-type RO systems and future potential: A review. *Desalination, 616*, Article 119404. https://doi.org/10.1016/j.desal.2025.119404
32. Kim, H.-W., Choi, W., Suh, D., Baek, Y., Cho, K., & Jeong, S. (2023). Pilot study of biofouling occurrence in a brackish water reverse osmosis system using intermittent operation. *Journal of Cleaner Production, 425*, 139097. https://doi.org/10.1016/j.jclepro.2023.139097
33. Lautenschlager, K., Boon, N., Wang, Y., Egli, T., & Hammes, F. (2010). Overnight stagnation of drinking water in household taps induces microbial growth and changes in community composition. *Water Research, 44*(17), 4868-4877. https://doi.org/10.1016/j.watres.2010.07.032

ISSN: 2181-3337 | SCIENTISTS.UZ

34. Lee, S., Cho, H., Choi, Y., & Lee, S. (2023). Application of optical coherence tomography (OCT) to analyze membrane fouling under intermittent operation. *Membranes, 13*(4), Article 392. https://doi.org/10.3390/membranes13040392
35. Lee, T., Choi, J. Y., & Cohen, Y. (2019). Gypsum scaling propensity in semi-batch RO (SBRO) and steady-state RO with partial recycle (SSRO-PR). *Journal of Membrane Science, 588*, Article 117106. https://doi.org/10.1016/j.memsci.2019.05.030
36. Li, M. (2026). Do membrane transport properties vary under dynamic and cyclic RO? Evidence for constant permeability and hysteresis from channel history. *Desalination, 620*, Article 119644. https://doi.org/10.1016/j.desal.2025.119644
37. Liang, Y. Y., & Li, M. (2026). Unsteady-state dynamics and AI in membrane desalination: Challenges and emerging opportunities. *Desalination, 618*, Article 119507. https://doi.org/10.1016/j.desal.2025.119507
38. Ling, F., Whitaker, R., LeChevallier, M. W., & Liu, W. T. (2018). Drinking water microbiome assembly induced by water stagnation. *The ISME Journal, 12*(6), 1520-1531. https://doi.org/10.1038/s41396-018-0101-5
39. Lu, X., Kujundzic, E., Mizrahi, G., Wang, J., Cobry, K., Peterson, M., Gilron, J., & Greenberg, A. R. (2012). Ultrasonic sensor control of flow reversal in RO desalination-Part 1: Mitigation of calcium sulfate scaling. *Journal of Membrane Science, 419-420*, 20-32. https://doi.org/10.1016/j.memsci.2012.05.027
40. Ma, M., Huang, B., Mei, L., Huang, K., Xing, K., & Liao, L. (2026). Development of a zero-stagnant-water purification system based on smart series-parallel control of dual RO membranes. *Membranes, 16*(5), Article 155. https://doi.org/10.3390/membranes16050155
41. Majamaa, K., Bertheas, U., Finlayson, F., & Levy, R. B. (2011). Preservation of reverse osmosis membranes with non oxidizing biocides - comparison with SMBS. *Water Supply, 11*(3), 342-351. https://doi.org/10.2166/ws.2011.041
42. Ogunniyi, E. O., & Richards, B. S. (2026). Renewable energy powered membrane technology: Resilient operating windows of a photovoltaic-powered desalination system operating under transient solar conditions. *Desalination, 625*, Article 119942. https://doi.org/10.1016/j.desal.2026.119942
43. Park, G. L., Schäfer, A. I., & Richards, B. S. (2011). Renewable energy powered membrane technology: The effect of wind speed fluctuations on the performance of a wind-powered membrane system for brackish water desalination. *Journal of Membrane Science, 370*(1-2), 34-44. https://doi.org/10.1016/j.memsci.2010.12.003
44. Park, G. L., Schäfer, A. I., & Richards, B. S. (2012). The effect of intermittent operation on a wind-powered membrane system for brackish water desalination. *Water Science and Technology, 65*(5), 867-874. https://doi.org/10.2166/wst.2012.912
45. Patel, C. G., Joshi, M., & Swaminathan, J. (2024). Membrane compaction in batch reverse osmosis operation and its impact on specific energy consumption. *Desalination, 592*, 118132. https://doi.org/10.1016/j.desal.2024.118132
46. Philibert, M., Villacorte, L. O., Ekowati, Y., Abushaban, A., & Salinas-Rodriguez, S. G. (2024). Fouling and scaling in reverse osmosis desalination plants: A critical review of membrane autopsies, feedwater quality guidelines and assessment methods. *Desalination, 592*(C), Article 118188. https://doi.org/10.1016/j.desal.2024.118188
47. Pomerantz, N., Ladizhansky, Y., Korin, E., Waisman, M., Daltrophe, N., & Gilron, J. (2006). Prevention of scaling of reverse osmosis membranes by "zeroing" the elapsed nucleation time. Part I. Calcium sulfate. *Industrial & Engineering Chemistry Research, 45*(6), 2008-2016. https://doi.org/10.1021/ie051040k

48. Ren, A., Dai, Z., Li, X., van der Meer, W., Rose, J. B., & Liu, G. (2025). Temperature-dependent microbial dynamics in touchless sensor faucets during short-term stagnation. *Environmental Science and Ecotechnology, 28*, Article 100624. https://doi.org/10.1016/j.ese.2025.100624
49. Richards, B. S., Capão, D. P. S., Früh, W. G., & Schäfer, A. I. (2015). Renewable energy powered membrane technology: Impact of solar irradiance fluctuations on performance of a brackish water reverse osmosis system. *Separation and Purification Technology, 156*, 379-390. https://doi.org/10.1016/j.seppur.2015.10.025
50. Richards, B. S., Capão, D. P. S., & Schäfer, A. I. (2008). Renewable energy powered membrane technology. 2. The effect of energy fluctuations on performance of a photovoltaic hybrid membrane system. *Environmental Science & Technology, 42*(12), 4563-4569. https://doi.org/10.1021/es703157n
51. Ruiz-García, A., & Nuez, I. (2020). Long-term intermittent operation of a full-scale BWRO desalination plant. *Desalination, 489*, Article 114526. https://doi.org/10.1016/j.desal.2020.114526
52. Sarker, N. R., & Bilton, A. M. (2021). Real-time computational imaging of reverse osmosis membrane scaling under intermittent operation. *Journal of Membrane Science, 636*, Article 119556. https://doi.org/10.1016/j.memsci.2021.119556
53. Sarker, N. R., Cherukupally, P., Sodhi, R., & Bilton, A. M. (2025). End-of-the-day rinsing for improved maintainability of intermittently operated small-scale photovoltaic-powered reverse osmosis systems. *Desalination, 599*, 118439. https://doi.org/10.1016/j.desal.2024.118439
54. Schäfer, A. I., Shen, J., & Richards, B. S. (2018). Renewable energy-powered membrane technology in Tanzanian communities. *npj Clean Water, 1*(1), Article 24. https://doi.org/10.1038/s41545-018-0026-6
55. Sitterley, K. A., Binger, Z., & Jenne, D. S. (2025). Comparing constant and transient membrane transport parameters for use in wave desalination models. *Membranes, 15*(8), Article 243. https://doi.org/10.3390/membranes15080243
56. Sitterley, K. A., Cath, T. J., Jenne, D. S., Yu, Y.-H., & Cath, T. Y. (2022). Performance of reverse osmosis membrane with large feed pressure fluctuations from a wave-driven desalination system. *Desalination, 527*, Article 115546. https://doi.org/10.1016/j.desal.2022.115546
57. Torii, S., Hashimoto, T., Do, A. T., Furumai, H., & Katayama, H. (2019). Impact of repeated pressurization on virus removal by reverse osmosis membranes for household water treatment. *Environmental Science: Water Research & Technology, 5*(5), 910-919. https://doi.org/10.1039/C8EW00944A
58. Tow, E. W., Wei, Q. J., Abraham, A. R., Chua, K. L., Plumley, M. J., & Lienhard, J. H. (2025). Piloting batch reverse osmosis with a flexible bladder for water recovery from scaling-prone brine. *npj Clean Water, 8*, Article 30. https://doi.org/10.1038/s41545-025-00462-6
59. Tu, K. L., Chivas, A. R., & Nghiem, L. D. (2014). Effects of chemical preservation on flux and solute rejection by reverse osmosis membranes. *Journal of Membrane Science, 472*, 202-209. https://doi.org/10.1016/j.memsci.2014.08.052
60. Uchymiak, M., Bartman, A. R., Daltrophe, N., Weissman, M., Gilron, J., Christofides, P. D., Kaiser, W. J., & Cohen, Y. (2009). Brackish water reverse osmosis (BWRO) operation in feed flow reversal mode using an ex situ scale observation detector (EXSOD). *Journal of Membrane Science, 341*(1-2), 60-66. https://doi.org/10.1016/j.memsci.2009.05.039
61. Valladares Linares, R., Wexler, A. D., Bucs, S. S., Dreszer, C., Zwijnenburg, A., Flemming, H. C., Kruithof, J. C., & Vrouwenvelder, J. S. (2016). Compaction and relaxation of biofilms. *Desalination and Water Treatment, 57*(28), 12902-12914. https://doi.org/10.1080/19443994.2015.1057036
62. Van Buggenhout, S., Verbeke, R., Davenport, D. M., & Vankelecom, I. F. J. (2025). Drying polymer membranes for preservation: A review. *Journal of Membrane Science, 731*, Article 124190. https://doi.org/10.1016/j.memsci.2025.124190

ISSN: 2181-3337 | SCIENTISTS.UZ

63. Warsinger, D. M., Tow, E. W., Maswadeh, L. A., Connors, G. B., Swaminathan, J., & Lienhard, J. H. (2018). Inorganic fouling mitigation by salinity cycling in batch reverse osmosis. *Water Research, 137*, 384-394. https://doi.org/10.1016/j.watres.2018.01.060
64. Wu, J., He, J., Quezada-Renteria, J. A., Le, J., Au, K., Guo, K., Xiao, M., Wang, X., Dlamini, D., Fan, H., Pataroque, K., Suleiman, Y., Shahbazmohamadi, S., Elimelech, M., Li, Y., & Hoek, E. M. V. (2024). Polyamide reverse osmosis membrane compaction and relaxation: Mechanisms and implications for desalination performance. *Journal of Membrane Science, 706*, Article 122893. https://doi.org/10.1016/j.memsci.2024.122893
65. Wu, J., He, J., Quezada-Renteria, J. A., Xiao, M., Le, J., Au, K., Guo, K., Ye, N., Toma, T., Elimelech, M., Li, Y., & Hoek, E. M. V. (2025). Role of transmembrane pressure and water flux in reverse osmosis composite membrane compaction and performance. *Environmental Science & Technology, 59*(17), 8856-8866. https://doi.org/10.1021/acs.est.5c02618
66. Yang, H., Choi, J., Choi, Y., & Lee, S. (2022). Effect of intermittent operation modes on performance of reverse osmosis (RO) membrane in desalination and water treatment. *Membrane and Water Treatment, 13*(1), 39-49. https://doi.org/10.12989/mwt.2022.13.1.039
67. Yin, Y., & Huang, H. (2026). Membrane-based decentralized water supply systems for rural population: A critical review. *Journal of Environmental Management, 405*, Article 129727. https://doi.org/10.1016/j.jenvman.2026.129727
68. Zhang, B., Jiang, Y., Fang, F., & Zhang, K. (2019). Membrane fouling in reverse-osmosis filters during real drinking water purification: Impact of operation modes and pretreatment. *Desalination and Water Treatment, 159*, 214-223. https://doi.org/10.5004/dwt.2019.24058
69. Zlatanović, L., van der Hoek, J. P., & Vreeburg, J. H. G. (2017). An experimental study on the influence of water stagnation and temperature change on water quality in a full-scale domestic drinking water system. *Water Research, 123*, 761-772. https://doi.org/10.1016/j.watres.2017.07.019

ISSN: 2181-3337 | SCIENTISTS.UZ